MONOCLINIC - TETRAGONAL ZIRCONIA QUANTIFICATION OF COMMERCIAL NANOPOWDER MIXTURES BY XRD AND DTA

M. R. GAUNA*, M. S. CONCONI*, S. GOMEZ*, G. SUÁREZ*, **, E. F. AGLIETTI*, **, #N. M. RENDTORFF*, **

*CETMIC, Centro de Tecnología de Recursos Minerales y Cerámica,
Camino Centenario y 506, M.B.Gonnet, Buenos Aires, Argentina
**Dpto de Química. Facultad de Ciencias Exactas, Universidad Nacional de La Plata,
1 y 115 La Plata, Buenos Aires, Argentina

#E-mail: rendtorff@cetmic.unlp.edu.ar

Submitted August 19, 2015; accepted October 20, 2015

Keywords: Zirconia, Nanopowders, XRD, DTA

The phase quantification in ceramic nanopowders presents technological interest for studying and design purposes. Especially in zirconia ceramics where the mechanical and transport properties are strongly affected by the crystalline composition. In this work we present the comparison XRD based methods and differential thermal analysis methods for phase characterization and specially quantification.

A complete series of commercial nanopowders mixtures (D50 ≈ 0.1 μm) of monoclinic zirconia (m) and partially stabilized zirconia (t: 3 % yttrium oxide) was studied. X ray diffraction (XRD) was performed and the relation m:t was quantified by the so called Garvie-Nicholson (G-N), Toraya and Rietveld method.

A complete reversible DTA analysis was carried out to the same mixtures. Both m-t and t-m martensitic thermal transformations were observed and pondered for the m-ZrO_2 containing samples. The graphical integration was performed and employed for the construction of a calibration curve in the studied composition range.

The results were compared, the Toraya method presented equivalent results in comparison with the Rietveld method. The G-N method presented appreciable differences (≈ 10 %). To assume a direct proportion of the m-ZrO_2 content with the peak area resulted in important errors but if a simple calibration curve is constructed, the DTA method presents accurate quantification with results comparable to the best XRD based quantification.

INTRODUCTION

Zirconia (ZrO_2) is derived from zircon and baddeleyite in nature, and it has three polymorph forms depending on various temperatures. Monoclinic ZrO_2 (m-ZrO_2) exists at temperatures lower than 1170°C. Tetragonal ZrO_2 (t-ZrO_2) exists between 1170 and 2370°C. When temperatures are higher than 2370°C, the phase transition from t-ZrO_2 to cubic ZrO_2 (c-ZrO_2) occurs [1-4]. However by usually several cations as Ca^{2+}, Mg^{2+}, Y^{3+}, Ce^{4+}, etc. fully cubic or partially tetragonal phases can by stabilized at room temperature. Zirconias are important ceramic materials for a broad range of applications. The traditional applications of ZrO_2 are use as refractory ceramics and abrasion-resistant materials, biomaterials [5-6]. In addition, due to the fact that ZrO_2 possesses the properties of high strength and toughness, good wear resistance, hardness, and thermal shock resistance, it has many engineering applications, such as use in automobile engine parts, exhaust parts, brake parts and cutting tools [1]. Moreover, also ZrO_2 is an appropriate material for thermal barrier coatings on metal components because it has a relatively high thermal expansion coefficient (compared to many other ceramics) and low thermal conductivity [3-10].

Monoclinic to tetragonal change in Zirconia is known as martensitic transformation and occurs around 1170°C in heating and 800°C in cooling presenting a significant volume change and a shear strain of ≈ 4 % and ≈ 0.16 % respectively. If not controlled, the volume change can result in fractures and, therefore, structural unreliability of fabricated components [11-12].

In materials design the phase quantification is an important tool for both designing and control. Quantification of these phases can be done following two different principles, crystallographic and differential thermal analysis [13-16].

The relation between atomic structure, macroscopic properties and final material behavior constitute a target for material science, particularly in the design and development of ceramic materials. For these a deep study of the crystalline composition is important to understand the final behavior of the material.

In zirconia ceramics systems, the monoclinic tetragonal relation is important to understand for example the mechanical and thermo mechanical behaviors and other properties like catalytic activity [3].

Different strategies for phase quantification have been developed. Like Raman spectroscopy [17-20], neutron diffraction [21], hyperfine interacions [22], X ray

absortion [23-25]. Particularly the X ray diffraction (XRD) is one of the common techniques for crystalline phase identification. Three different XRD methods are usually employed in Zirconia materials design and characterization, two of them based on semi-empirical calculations (Garvie-Nicholson [26] and Toraya [27]) and the complete profile refinement iterative Rietveld method [28-32]. The last being an effective analytical tool for quantitative phase analysis on various materials. Some attempts for the three more important polymorphs have been also made but are more difficult to implement [33], and on top of that is difficult to find the three polymorphs in the same sample.

Recently Arata et al. successfully evaluated the aging evolution of a zirconia dental material by the Rietveld method and demonstrated that the G-N presents some problems with the cubic zirconia pondering, and that is an error to assume equivalence with the tetragonal phase diffraction intensities, in fact t/c peaks could be solved in their patterns [34].

In recent works we proved that the TMA the *m-t-m* loop area in the reversible thermal cycle over the transformation temperature is proportional to the *m*-zirconia content in a dispersoidal ceramic composite [35-36].

In a series of articles focused in zirconia containing composites we succeeded to estimate the amount of zirconia in terms of the perturbed angular correlations method (PAC) [37-39]. Similar approach was carried out for some milled zirconia-ytriananopowders of the [40]. Not only m and t phases were evaluated and ponderated, but the experimental difficulty of this technique, implying neutron activated samples makes it difficult for rapid feedback in materials development, from this point of view the XRD advantages are evident, the thermal analysis similar, both techniques are inexpensive and usually available in ceramics laboratories.

Is evident that different ways for phase quantitation are being used in literature but few discussions about their accuracy exist, especially in nano sized powders.

Zirconia ceramic exhibits a phase transformation between monoclinic and tetragonal phases. It can be seen that most of the reported *m-t* and *t-m* temperatures are in the temperature range 1400-1480 and 1250-1325 K, respectively [35]. DTA zirconia materials were extensively reviewed by Wang et al. [7] the different reported experimental data from the *m-t* transition was listed. While the *m-t* peak is an endothermic symmetrical Gaussian"like" peak, the *t-m* consists in an unsymmetrical peak, with an abrupt left side. As expected the peak areas (*m-t* and *t-m*) are generally equivalent and should be directly proportional to the m-zirconia content in the sample. This fact supports the hypothesis of employing the area integral for quantifying the monoclinic content, which is the proposed methodology using thermal analysis.

In this work a whole series of commercial nanopowders mixtures of monoclinic and partially stabilized zirconia powders were prepared in order to evaluate and discuss the mentioned analytical techniques (based on the XRD pattern treatment and the DTA), their accuracy and inherent errors.

EXPERIMENTAL

Materials and samples preparation

The materials used in the present work were commercials nanopodwers. Pure monoclinic Zirconia (*m*-ZrO_2: MZ, Tosoh Corporation, Tokyo, Japan.) and 3 mol. % Yttria-Partially-Stabilized tetragonal Zirconia (PSZ, Tosoh Corporation, Tokyo, Japan.) with specific surface of 14 and 16 ($m^2 \cdot g^{-1}$) respectively and $D_{50} \approx 0.1$ μm for both powder.

SEM images (Scanning electron microscope: SEM Quanta FEI) of both powders are shown in Figure 2. Clearly in both cases microstructure is homogeneous. Grains present a rounded shape and a monomodal particle size distribution of approximately 80 nm can be seen.

Different mixtures were intimately mixed in ethanol, stirred and homogenized in an ultrasonic bath. Four intermediate successive equidistant mixtures were prepared as shown in Table 1. Finally the mixtures were dried (110°C) and studied.

Table 1. Different MZ and PSZ nanopowders mixtures composition.

Mixture	MZ (wt. %)	PSZ (wt. %)
m_{100}-t_0	100	0
m_{80}-t_{20}	80	20
m_{60}-t_{40}	60	40
m_{40}-t_{60}	40	60
m_{20}-t_{80}	20	80
m_0-t_{100}	0	100

Zirconia nanopowders characterizations

The nanopowders were characterized by X-ray diffraction (XRD, Philips PW 3710 with Kα: Cu as incident radiation and Ni filter). The equipment was operated at 40 kV and 35 mA and the scanning was performed with a step of 0.04° and 2 s per step in the range between 2θ = 10 - 80°. The dried powders were studied and analyzed in aluminum sample holders. A punctual scintillation detector was employed. The set of divergence, receiving and scattering slits were 1°, 0.2°, 1° and in this study no monochromator was used.

The Differential Thermal Analysis (DTA) and Thermogravimetric (TG) were recorded simultaneously with the equipment Netzsch STA 409C in the temperature

range between 25-1400-100°C using reversible mode with heating rate of 10°C·min^{-1}. Oxidizing atmosphere were used by introducing analytical air and using alumina crucibles and calcinated alumina (Al_2O_3) as reference.

XRD pattern treatments

Garvie Nicholson (G-N) method is based in X-ray diffraction and estimate the *m*-ZrO_2 and *t*-ZrO_2 content from the relations of intensities of the reflections in the diffraction pattern according the following equations:

$$Im\ (111) + Im\ (\bar{1}11) = It\ (101) \quad (1)$$

The molar fraction of the content of m-ZrO_2 is given by:

$$Xm = \frac{Im\ (111) + Im\ (\bar{1}11)}{Im\ (111) + Im\ (\bar{1}11) + It\ (101)} \quad (2)$$

Being *Im* (111) and *Im* ($\bar{1}$11) the intensity of the monoclinic phase for the peak corresponding to planes 111 and ($\bar{1}$11) respectively. It (101) corresponds to the intensity of the 101 plane.

The so called Toraya method is also based in only some peak intensity values. This technique estimates the volumetric fractions of the *m*-ZrO_2 (*Vm*) and *t*-ZrO_2 (*Vt*) phases from the intensities of the diffraction peaks ($\bar{1}$11) and (111) of *m*-ZrO_2 and line diffraction (101) *t*-ZrO_2 as:

$$Vm = \frac{1.311x}{1+0.311x} \quad (3)$$

where,

$$x = \frac{Im\ (\bar{1}11) + Im\ (111)}{Im\ (\bar{1}11) + Im\ (111) + It\ (101)} \quad (4)$$

The tetragonal fraction (*Vt*) is given by:

$$Vt = 1 - Vm \quad (5)$$

The third and more accurate method is the known as the Rietveld method devised by Hugo Rietveld for use in the characterization of crystalline materials. Uses a least squares approach to refine a theoretical line profile until it matches the measured profile. The introduction of this technique was a significant step forward in the diffraction analysis of powder samples as, unlike other techniques at that time; it was able to deal reliably with strongly overlapping reflections. The method was first reported for the diffraction of monochromatic neutrons where the reflection-position is reported in terms of the Bragg angle 2θ [28].

Quantitative Phase Analysis (sometimes called also Standardless Phase Analysis, Multiphase Rietveld Phase Quantification, Rietveld Quantitative Analysis or Rietveld XRD Quantification) is a powerful method for determining the quantities of crystalline and amorphous components in multiphase mixtures. This is quantitative analysis results from the refined scaling factors for each phase (S_i) according to the following equation:

$$W_i = \frac{S_i (ZMV)_i / \tau_i}{\sum_p S_p (ZMV)_p / \tau_p} \quad (6)$$

where, W_i is the weight fraction of the phase i, the sum is over all phases present and S_i, Z_i, M_i, V_i y τ_i are the scale factor, the number of molecules per unit cell, the molecular weight, the volume of the cell and the correction factor for mass absorption of the particles phase *i*, respectively. This method has proven to be an effective tool for quantitative analysis of phases in various materials [30-31], this requires knowing the crystal structure of each phase present in the sample

The advantages of Rietveld Quantitative Analysis are that the calibration constants are computed from reliable structural data, rather than by laborious expe-

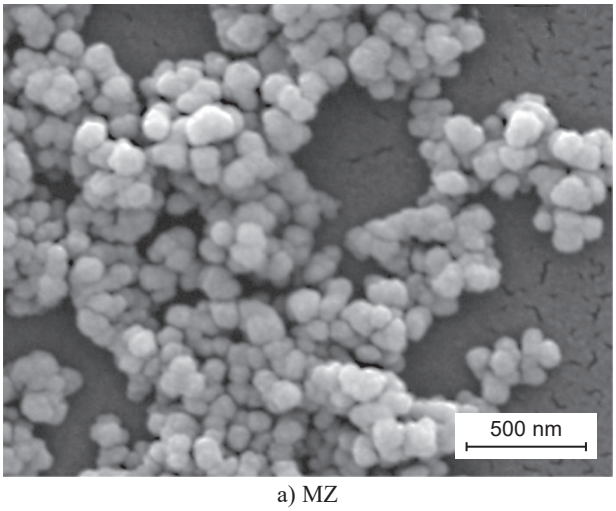

a) MZ

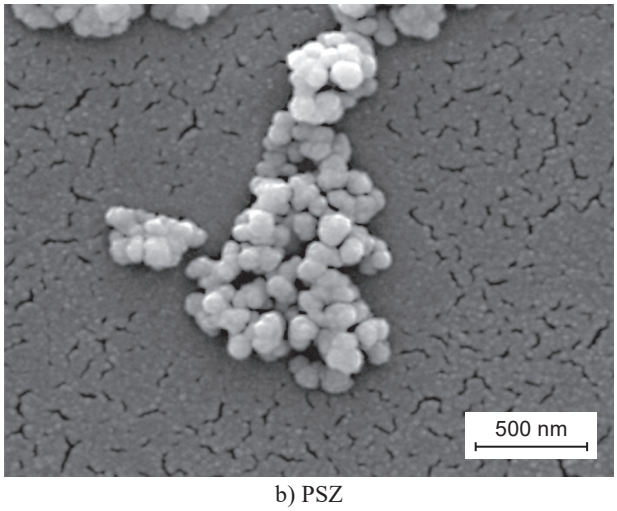

b) PSZ

Figure 1. SEM micrographs of the studied commercial nanopowders; a) MZ and b) PSZ.

riments, secondly all reflections in the pattern are explicitly included for calculation, the effects of preferred orientation and extinction are reduced, since all reflection types are considered as well. Finally the crystal structural and peak profile parameters, particle statistics, micro absorption, etc. are refined as part of the same analysis.

The sample analysis is performed using the program Fullprof [8]. It was assumed that the tetragonal phase corresponds to the space group $P4_2/nmc$ with cations Zr^{4+} and Y^{3+} in special positions 2a and anions O^{2-} in positions 4d and the monoclinic phase to the group $P2_1/c$ with ion Zr^{4+} and O^{2-} in general positions (x, y, z). The profile of the diffraction peaks was adjusted using a pseudo-Voigt function.

Zirconia nanopowder differential thermal analysis (DTA)

The progressive growth of the monoclinic to tetragonal DTA endothermic peak area with the amount of m-ZrO_2, is expected due to the nature of the transformation and the DTA analysis fundamentals, and will be employed for constructing a kind of calibration curve, this strategy in not odd in material science and particularly in ceramic materials [43]. This peak presents a Gaussean shape [7] which is an advantage over the unsymmetrical t-m exothermic one; however the same analysis could be performed. A Gaussean fit was performed to the peaks for complementing the study. Once built the calibration curve will be contrasted with the XRD quantifications performed.

RESULTS AND DISCUSSION

XRD analysis of the as received nanopowders

The as received commercial nano powders diffraction patterns are shown in Figure 2, the top right inset presents the detail (in the region between 27 and 33° (2θ)) of the overlapped patterns. As expected, the m_{100}-t_0 sample only presents the m-ZrO_2 peaks. On the other hand the m_0-t_{100} sample presents the t-ZrO_2 as the principal phase which is accompanied by the m-ZrO_2 peaks in a smaller proportion. Particularly in the inset the (111) and (-111) peaks for the monoclinic (m_{100}-t_0) phase and the (101) for the tetragonal (m_0-t_{100}) phase can be observed for both nanopowders

It is clearly seen that while the monoclinic Zirconia (m_{100}-t_0) present only peaks of the monoclinic phase, m_0-t_{100} presents both the peaks corresponding to the tetragonal and monoclinic phases.

Commercial PSZ (m_0-t_{100}) present also monoclinic peak because is partially stabilized. In fact, after the Rietveld quantification it was found that the amount of m-ZrO_2 is 32 % of the total zirconia. Over 1170°C these amount of monoclinic phase will transform in totally tetragonal Zirconia, but the monoclinic can be previously chemically stabilized (during a thermal treatment) in the presence of cations, by the cation migration, if there is diffusion pathways available like in activated or not fully crystalline phases, this kind of transformation do not present the mentioned endothermic peak and is not reversible [44-45].

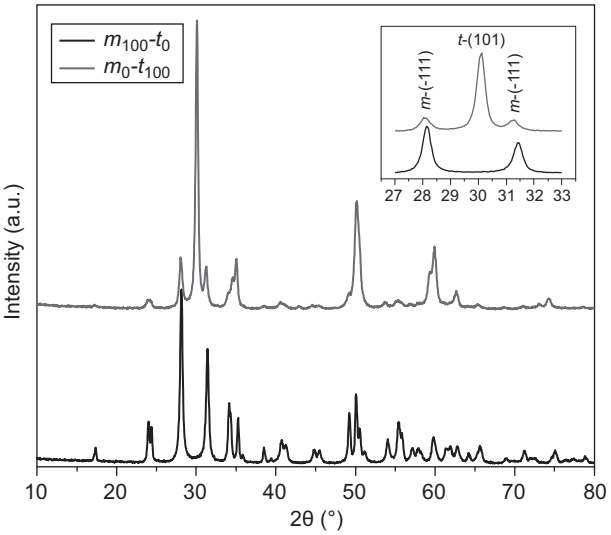

Figure 2. Diffraction patterns of the studied commercials nanopowders (m_{100}-t_0 pure monoclinic Zirconia and m_0-t_{100} PSZ).

Differential thermal analysis (DTA)

Differential Thermal Analysis was performed in order to observe the reversible martensitic transformation of m-ZrO_2 to t-ZrO_2. Figure 3 shows the DTA curves of the as received MZ and PSZ Zirconia (m_{100}-t_0) and (m_0-t_{100}) in a reversible heating cycle up to 1350°C.

The martensitic m to t transformation can be easily observed in the first powder, the endothermic negative peak beginnings at 1173°C, presents the critical point at

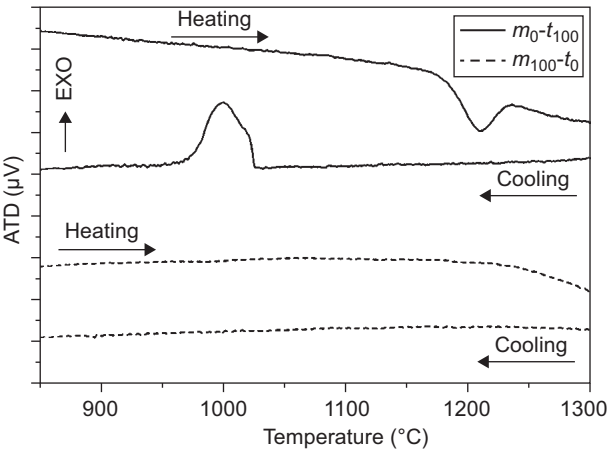

Figure 3. Differential thermal analysis: Reversible chart of the nanopowder MZ and PSZ.

1208°C and ends at 1236°C. The cooling curve present an exothermic peak, corresponding to the inverse transformation beginning at 1025°C, a maximum at 1000°C and ends at 963°C. The value of 1173°C for the monoclinic to tetragonal transformation is in concordant with literature as well 963°C [7].

On the other hand no evident peaks can be observed in the PSZ, this was unexpected due to the not negligible amount of *m*-ZrO_2 that was evaluated in this powder (28 wt. %) evidencing chemical stabilization.

XRD analysis of the zirconia nano powders mixed polymorphs

Figure 4 shows the XRD patterns of the series of prepared samples. Samples were vertically translated for better observation. In the top right inset the detail of the overlapped patterns can be observed in the G-N and Toroya zone.

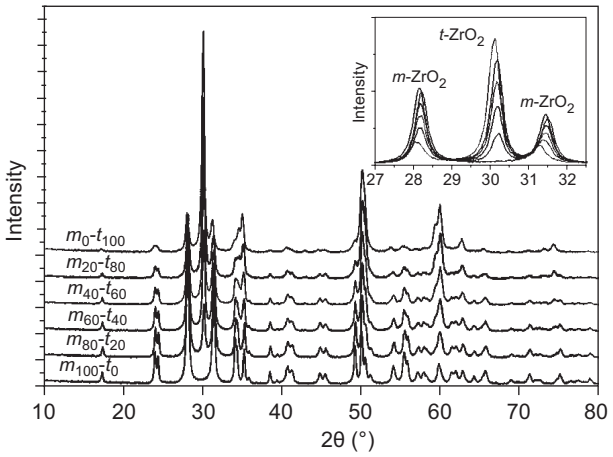

Figure 4. XRD patterns of the samples m_0-t_{100} to m_{100}-t_0.

A Rietveld refinement was performed for the series of patterns. The results of the refinement can be observed in Table 2. The adequate goodness of the performed refinements arises from the Rwp values, it is important to keep in mind that the profiles obtained are typical of the zirconia nanopowders, in terms of peak width and intensities. The accuracy of the cell parameters would be affected by this fact. The results of the Rietveld based phase quantification is shown in Table 3. Afterward from the respective peak intensities (numerical integral), the two semi-empirical described methods were carried out; the results are shown in Table 3 as well.

Table 3 shows the estimated values of m-ZrO_2 content by G-N and Toroya methods and the Rietveld refinement method. Assuming that the Rietveld results is the true one, the accuracy of the Toroya method is remarkable the observed differences are neglect able, on the other hand the results of the classical and more simple G-N method underestimates the amount of monoclinic phase (over estimates the amount of the tetragonal proportion) in the phase quantification in these nanopowders. The observed errors are in some case over 10% in relative basis. In conclusion the G-N method is only recommendable for a rapid quantification.

Table 3. Results the semi-empirical quantifications (Garvie Nicholson and Toraya) and Rietveld based quantification.

	Garvie-Nicholson		Toraya		Rietveld	
Samples	*m*-ZrO_2	*t*-ZrO_2	*m*-ZrO_2	*t*-ZrO_2	*m*-ZrO_2	*t*-ZrO_2
m_{100}-t_0	100	0	100	0	100	0
m_{80}-t_{20}	80	20	84	16	84.0	16.0
m_{60}-t_{40}	64	36	70	30	70.4	29.6
m_{40}-t_{60}	52	48	58	42	58.4	41.6
m_{20}-t_{80}	40	60	46	54	45.8	54.2
m_0-t_{100}	28	72	33	67	32.7	67.3

Table 2. Rietveld refinement results.

	ICSD	a	Error	b	Error	c	Error	α	Error	β	Error	g	Error	Rwp
MZ	26488	5.1690	–	5.232	–	5.341	–	90	–	99.25	–	90	–	–
PSZ	62994	3.6055	–	3.606	–	5.18	–	90	–	90	–	90	–	–
Sample	Phase													
m_0-t_{100}	*m*	5.1570	0.0040	5.2040	0.0009	5.3140	0.0008	90	0	98.910	0.009	90	0	11.4
	t	3.6070	0.0010	3.6070	0.0010	5.1660	0.0004	90	0	90.000	0	90	0	–
m_{20}-t_{80}	*m*	5.1490	0.0030	5.2071	0.0008	5.3081	0.0007	90	0	99.056	0.008	90	0	12.2
	t	3.6080	0.0010	3.6080	0.0010	5.1670	0.0004	90	0	90.000	0	90	0	–
m_{40}-t_{60}	*m*	5.1460	0.0030	5.2077	0.0006	5.3080	0.0006	90	0	99.129	0.007	90	0	13.7
	t	3.6080	0.0010	3.6080	0.0010	5.1684	0.0005	90	0	90.000	0	90	0	–
m_{60}-t_{40}	*m*	5.1450	0.0030	5.2090	0.0006	5.3090	0.0006	90	0	99.164	0.006	90	0	15.9
	t	3.6090	0.0020	3.6090	0.0020	5.1691	0.0007	90	0	90.000	0	90	0	–
m_{80}-t_{20}	*m*	5.1447	0.0005	5.2086	0.0006	5.3093	0.0006	90	0	99.194	0.005	90	0	18.7
	t	3.6108	0.0006	3.6108	0.0006	5.171	0.0010	90	0	90.000	0	90	0	–
m_{100}-t_0	*m*	5.1460	0.0030	5.2103	0.0006	5.3106	0.0006	90	0	99.214	0.007	90	0	23.2

Differential thermal analysis (DTA) of the zirconia nanopowders and mixtures

Figure 5 shows the DTA peak for the six studied samples and Table 4 shows the properties of mentioned peaks together with the gaussean fitting results. From these, the gaussean shape is evident and the gradual area increase. The position, width and FWHM of the peaks are similar to the once reported in literature [7]. The small differences in the initial temperature observed are attributed to the low amount of m-ZrO_2.

A remarkable result is the absence of endothermic peak in the PSZ nanopowder (m_0-t_{100}). This fact might be explained by the chemical, cation based stabilization of the former m-ZrO_2 into t-ZrO_2 before this temperature range. The powder presents nanocrystalline structure and certain amount of Ytrium oxide. In order to eluci-date this issue, an XRD analysis of a thermally treated (1350°C) sample, of MZ (m_0-t_{100}), was carried out. No m-ZrO_2 peaks were detected, the only crystalline manifestations corresponded to the t-ZrO_2, sustaining that the Badelleyite was irreversibly stabilized during the thermal processes.

Employing the Rietveld quantification results and the Peak integral (graphical) area the calibration curve can be easily constructed. This is shown in Figure 6 in solid red. The results of the linear fit are shown as well. The linear behavior is evident. The residual values were in all the cases below 2 % showing the accuracy of employing the calibration curve in the complete concentration range. On the other hand if no calibration curve is build and the proportionality with the pure m-ZrO_2, is assumed, a great underestimation would be the result; especially at low m-ZrO_2 concentration as it can be observed in the difference between the red line and the dashed line, this methodology should be discarded.

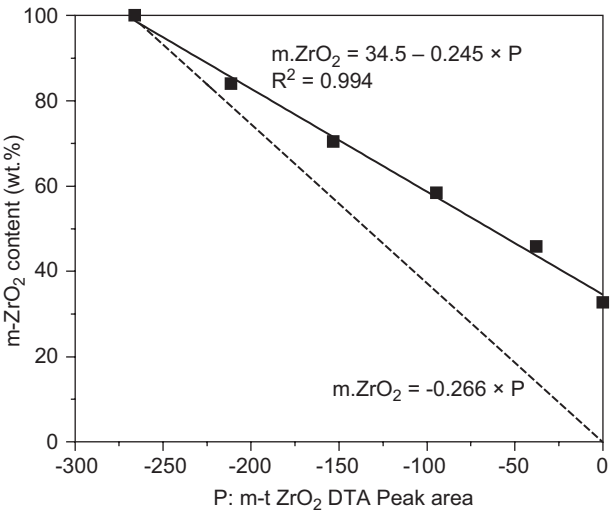

Figure 6. Calibration curve build with the endothermic m-t zirconia transformation peak and the XRD-Rietveld quantification of the m-ZrO_2.

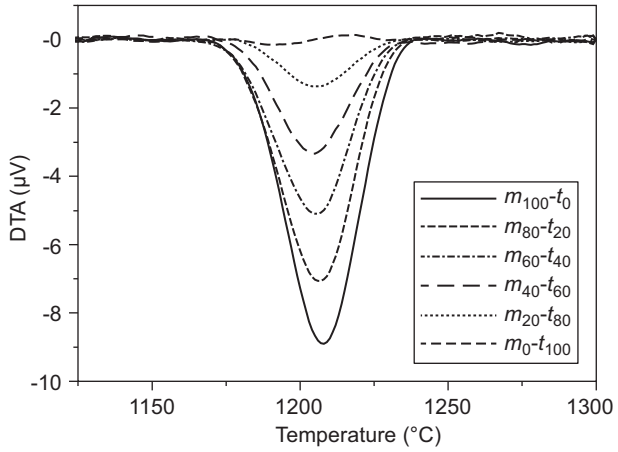

Figure 5. DTA curves detail in the 1100-1300°C range in the heating semi cycle of the studied zirconia commercial Nano powders.

Comparison of the different studied methods

In order to compare the studied techniques in Figure 7 the results of the XRD semi-empirical and the two DTA approaches (Zi) are plotted as a function of the Rietveld refinement m-ZrO_2 quantification results (Zr). The full black line corresponds to the line with slope one, the difference between Zi and Zr is plotted in the left inset of Figure 7.

The accuracy can be compared from this plot; the accuracy of the DTA method with calibration curve is comparable to the excellent behavior of Toraya method: a semi empirical method function of the principal diffraction peaks of m and t polymorphs, differences. The Garvie Nicholson method, also semi empirical but with

Table 4. Peak properties and Gaussean fit results of the m-t endothermic DTA peak.

Mixture	Peak integral	Temperature (°C)			Gaussean peak integral	FWHM	Gaussean fit goodness R^2
		Initial	Maximum	Final			
m_{100}-t_0	-266.1	1173	1208	1236	-268.37	28.24	0.998
m_{80}-t_{20}	-211.2	1175	1207	1235	-217.07	28.50	0.997
m_{60}-t_{40}	-153.3	1173	1207	1235	-155.15	28.48	0.997
m_{40}-t_{60}	-94.6	1173	1206	1234	-96.40	27.12	0.996
m_{20}-t_{80}	-37.8	1180	1204	1233	-37.32	25.46	0.994
m_0-t_{100}	not observed		1200-1210		not fitted	not fitted	not fitted

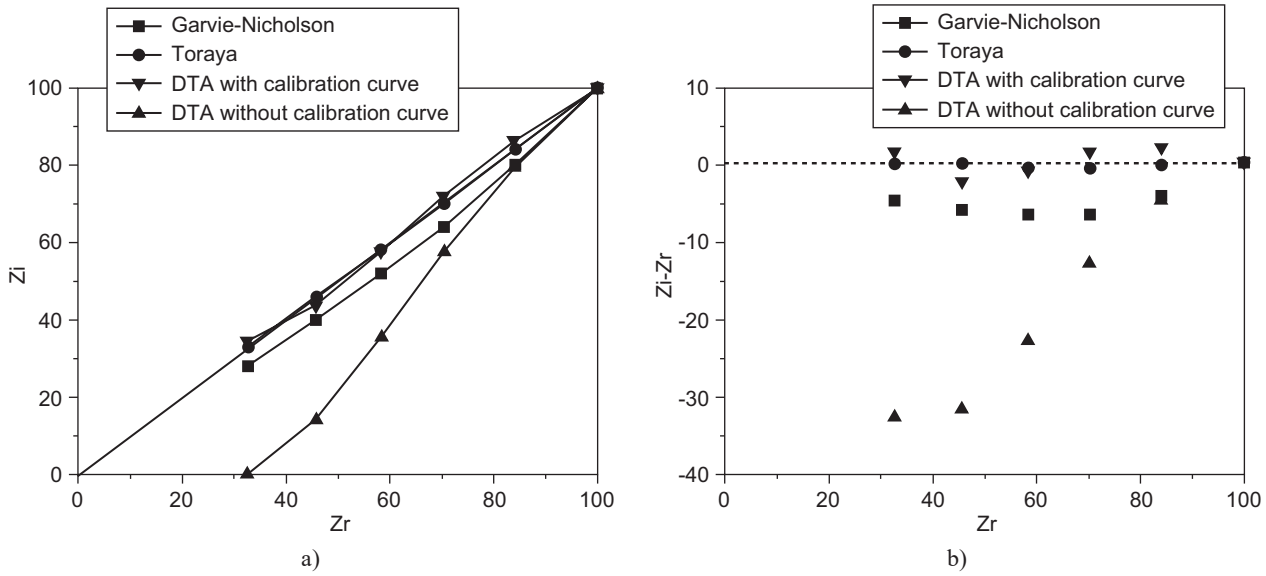

Figure 1. a) Monoclinic zirconia content (studied methods (Zi)) as a function of the zirconia evaluated by the Rietveld method (Zr); b) Differences between methods (Zi-Zr) as a function of the zirconia content (Zr).

a direct relation within the diffraction peaks, presents rough accuracy, in relative basis the error is in some cases over 10 %. However this could be recommended for rough quantification in the m-t ZrO_2 nano-powder systems.

Finally from the carried out analysis it can be concluded that the DTA analysis cannot be employed assuming a direct proportionality with the pure *m*-ZrO_2 peak area without a calibration curve this approach introduced up to ≈ 35 % of error. However if a simple calibration curve is constructed with the intensities of the endothermic monoclinic to tetragonal DTA peak an excellent accuracy is achieved.

CONCLUSIONS

The monoclinic and tetragonal phases are widely used as reinforcement of materials by martensitic transformation or microcraks formation. For these it is important to be able to measure adequately the phases content in complex mixtures with available technique as X-ray diffraction (XRD) and differential thermic analysis (DTA).

The aim of this study was to use and compare different techniques for Zirconia phase quantifications using XRD and DTA. Different monoclinic and tetragonal Zirconia mixtures prepared with commercial nanopodwers were characterized measuring morphology and particle size by SEM, and phase transformations with differential thermal analysis (DTA). Also the phases quantification was followed by DTA analysis and using three different XRD methods: Toraya, Garvie-Nicholson (G-N), and Rietveld refinement method.

The semi-empirical method of Garvie-Nicholson showed to by only suitable for quick phase comparison, on the other hand the Toraya methodology, also empirical, obtained excellent correspondence with the Rietveld based quantification.

Finally the methodology based in the thermal behavior (DTA) of the nanopowders mixture was only adequately accurate when a previous calibration curve was constructed with well-known mixtures, the direct m-t exothermic peak integral usage is not recommended, especially for low monoclinic content mixtures.

REFERENCES

1. Zender, H.H., Leistner, H., Searle, H.R. : Interceram *39*, 33 (1990).
2. Chevalier, J., Gremillard, L., Virkar, A.V., Clarke, D.R.: Journal of the American Ceramic Society *92*, 1901 (2009).
3. Hisbergues, M., Vendeville, S., Vendeville, P.: Journal of Biomedical Materials Research – Part B Applied Biomaterials *88*, 519 (2009)
4. Vasylkiv, O., Sakka, Y.: Journal of the American Ceramic Society *84*, 2489 (2001).
5. Niihara, K.: Journal of the Ceramic Society of Japan *99*, 974 (1991).
6. Sternitzke, M.: Review: Journal of the European Ceramic Society *17*, 1061 (1997).
7. Wang, C., Zinkevich, M., Aldinger, F.: Journal of the American CeramicSociety *89*, 3751 (2006).
8. Bisson, J.-F., Fournier, D., Poulain, M., Lavigne, O., Mévrel, R.: Journal of the American Ceramic Society *83*, 1993 (2000).
9. Torralvo, M.J., Alario, M.A., Soria, J.: Journal of Catalysis *86*, 473 (1984).
10. Chen, D.-J., Mayo, M.J.: Journal of the American Ceramic Society *79*, 906 (1996).

11. Ohji, T., Jeong, Y.-K., Choa, Y.-H., Niihara, K.: Journal of the American Ceramic Society *81*, 1453 (1998).
12. Kelly, P.M., Rose, L.R.F.: Progress in Materials Science *47*, 463 (2002).
13. Garvie, R.C.: Journal of Physical Chemistry *69*, 1238 (1965).
14. Garvie, R.C., Nicholson, P.S.: J. Am. Ceram. Soc. *55*, 303 (1972).
15. Scott, H.G.: Journal of Materials Science *10*, 1527 (1975).
16. Garvie, R.C.: Journal of Physical Chemistry *82*, 218 (1978).
17. Kontoyannis, C.G., Orkoula, M.: Journal of Materials Science *29*, 5316 (1994).
18. Muñoz Tabares, J.A., Anglada, M.J.: Journal of the American Ceramic Society *93*, 1790 (2010).
19. Boulc'h, F., Djurado, E.: Solid State Ionics *157*, 335 (2003).
20. Sheng, Tan Kha, Ramalingam, P.: Proceedings of SPIE - The International Society for Optical Engineering *4221*, 454 (2000).
21. Baldinozzi, G., Simeone, D., Gosset, D., Dutheil, M.: Physical Review Letters *90*, 2161031 (2003).
22. Caracoche, M.C., Dova, M.T., López García, A.R., Martínez, J.A., Rivas, P.C. : Hyperfine Interactions *39*, 117 (1988).
23. Fábregas, I.O., Lamas, D.G., Acua, L.M., De Reca, N.E.W., Craievich, A.F., Fantini, M.C.A., Prado, R.J. : Powder Diffraction 23, S46 (2008).
24. Fábregas, I.O., Lamas, D.G., Walsöe De Reca, N.E., Fantini, M.C.A., Craievich, A.F., Prado, R.J. : Journal of Applied Crystallography *41*, 680 (2008).
25. Acũa, L.M., Lamas, D.G., Fuentes, R.O., Fábregas, I.O., Fantini, M.C.A., Craievich, A.F., Prado, R.J. : Journal of Applied Crystallography *43*, 227 (2010).
26. Garvie, Ronald C., Nicholson, Patrick S. : Journal of the American Ceramic Society *55*, 303 (1972).
27. Toraya H., Yoshimura M., Somiya S. : J. Am. Ceram. Soc. *67,* C119 (1984).
28. Rietveld H.M.: J. Appl. Crystallogr. *2*, 65 (1969).
29. Young R.A.: *The Rietveld method*, IUCr, Oxford University Press, New York, 1995.
30. Bish, D.L., Post, J.E.: American Mineralogist *78*, 932 (1993).
31. Conconi M. S., Rendtorff N. M., Aglietti E. F. : New Journal of Glass and Ceramics *1*, 28 (2011).
32. Rodríguez - Carvajal, J.: Physica B *92*, 55 (1993).
33. Schmid, H. K.: Journal of the American Ceramic Society *70*, 367 (1987)
34. Arata, A., Campos, T. M. B., Machado, J. P. B., Lazar, D. R. R., Ussui, V., Lima, N. B., Tango, R. N.:. Journal of dentistry *42*, 1487 (2014).
35. Rendtorff, N. M., Garrido, L. B., Aglietti, E. F.: Journal of thermal analysis and calorimetry *104*, 569 (2011).
36. Rendtorff, N. M., Suarez, G., Sakka, Y., Aglietti, E. F.: Journal of thermal analysis and calorimetry *110*, 695 (2012).
37. Rendtorff, N.M., Conconi, M.S., Aglietti, E.F., Chain, C.Y., Pasquevich, A.F., Rivas, P.C., Martínez, J.A., Caracoche, M.C.: Hyperfine Interactions *198*, 219 (2010).
38. Rendtorff, N.M., Conconi, M.S., Aglietti, E.F., Chain, C.Y., Pasquevich, A.F., Rivas, P.C., Martínez, J.A., Caracoche, M.C.: Hyperfine Interactions *198*, 211 (2010).
39. Chain, C.Y., Pasquevich, A.F., Rivas, P.C., Martínez, J.A., Caracoche, M.C., Rendtorff, N.M., Conconi, M.S., Aglietti, E.F.: Hyperfine Interactions *198*, 61 (2010).
40. Rendtorff, N.M., Suárez, G., Aglietti, E.F., Rivas, P.C., Martinez, J.A.: Ceramics International *39*, 5577 (2013).
41. Rodríguez-Carvajal, J. : Newsletter *26*, 12 (2001).
42. Bansal, N.P., Boccaccini, A.R.: Ceramics and Composites Processing Methods 585 (2012).
43. Rhodes, W.H., Carter, R.E.: J. Am. Ceram. Soc. 49, (1966).
44. Michel D., Faudot F., Gaffet E., Mazerolles L.: Journal of the American Ceramic Society *76*, 2884 (1993).